J. Physiol. (1977), **264**, *pp.* 163–198
With 1 plate and 11 text-figures
Printed in Great Britain

THE OPTICAL PROPERTIES OF BIREFRINGENCE SIGNALS FROM SINGLE MUSCLE FIBRES

BY S. M. BAYLOR AND H. OETLIKER

From the Department of Physiology, Yale University School of Medicine, New Haven, Connecticut 06510, U.S.A., and the Department of Physiology, University of Bern, and Schule für Biologie Laboranten, Wander, Bern, Switzerland

(*Received 17 May 1976*)

SUMMARY

1. The optical retardation of single muscle fibres at rest and the optical properties of the large, early birefringence signal detectable during a twitch (Baylor & Oetliker, 1975, 1977*a*) were investigated.

2. The resting birefringence, B, which is the factor relating resting retardation, R, to the light path length through the fibre, L, was found to be $2{\cdot}25 \times 10^{-3}$ (i.e. $R = 2{\cdot}25 \times 10^{-3} \times L$) and to be independent of wave-length (λ = 480–660 nm).

3. When the angle of incidence, ψ, of the crossed polarizers with respect to the fibre axis was varied, the resting light intensity and large, early change in light intensity were related by the function $\sin^2\psi . \cos^2\psi$. When the net phase shift, ϕ_λ, of a narrow longitudinal strip of fibre plus compensator was varied, the resting light intensity was described by the function $(1 - \cos\phi_\lambda)$, whereas the early change in light intensity followed $\sin\phi_\lambda$. These results make it likely that the optical mechanism underlying the early birefringence signal is a change in retardation.

4. When a narrow longitudinal strip of fibre was illuminated by monochromatic light in the range 480–690 nm, the magnitude of the signal varied approximately as expected if the retardation change is independent of wave-length.

5. The spatial characteristics of the signal were examined by moving a small slit of light across the fibre width as well as by measuring the signal collected from the entire fibre width as a function of wave-length. The results from both experiments support the idea that the large, early change in retardation is due to a volume-related rather than surface-related structure.

6. Under the assumption that the retardation change is distributed as fibre volume, its average magnitude was calculated. For fibres in normal Ringer the peak of the early retardation change compared with resting is about $1{\cdot}7 \times 10^{-3}$, and for fibres in D_2O Ringer about $0{\cdot}7 \times 10^{-3}$.

INTRODUCTION

During the twitch of a single muscle fibre, a large birefringence signal can be detected beginning shortly after stimulation (Baylor & Oetliker, 1975, 1977*a*). Although the earliest detectable light intensity change is coincident with the rising phase of the surface action potential (Baylor & Oetliker, 1975), the main rising phase of the large optical signal clearly occurs after the peak of the action potential but before the development of tension (Baylor & Oetliker, 1975, 1977*a*, *b*). The time course and other physiological properties of this signal are consistent with the idea that it is related to events linking excitation to contraction. Further understanding of the possible origin of this signal is aided by an examination of the optical mechanism giving rise to it. The experiments and analysis of this paper are concerned with the determination of this information.

METHODS

The experimental methods were essentially those described in the previous paper (Baylor & Oetliker, 1977*a*). For the calculations in Tables 5 and 6, it was necessary to know the relative spectral variation of the output of the photodetector, independent of any variation due to the retardation introduced by the fibre. This function, denoted $S(\lambda)$, was approximated as follows. The source light was passed through the heat filters, then one of a series of twelve interference filters with peak transmittance at wave-length λ, and a narrow slit giving a bar of light at the level of the fibre that was smaller than a fibre diameter. The output function $T(\lambda)$ was first determined with only these components in the light path. Then at each wave-length, the fractional reduction in light intensity was determined when either (*a*) the polarizer, (*b*) the fibre, or (*c*) the analyser was introduced in the light path. If the fraction of light remaining in each case is called $R_a(\lambda)$, $R_b(\lambda)$, and $R_c(\lambda)$, then the function $S(\lambda)$ (Table 1) was obtained from

$$S(\lambda) \propto T(\lambda)\, R_a(\lambda)\, R_b(\lambda)\, R_c(\lambda)/[P(\lambda)\, D(\lambda)]$$

by arbitrarily setting the maximum value equal to unity.

$P(\lambda)$, the peak transmission (%) of the filter centred about wave-length λ, and $D(\lambda)$, the width of that filter (measured at 50 % peak transmission), were determined from the factory calibrations (Oriel). $D(\lambda)$ averaged 35 nm.

RESULTS

The resting retardation and birefringence

When a single fibre is positioned between a first polarizer oriented at $+45°$ and a second polarizer (analyser) oriented at $-45°$ with respect to the long axis of the fibre and illuminated with visible light of wave-length λ, it appears bright against a dark background (part *A* of the Plate). This is because a single fibre is quite transparent and inherently 'birefringent', i.e. the refractive index, n_e, for plane polarized light travelling through it

in the longitudinal plane (0°) is different from the refractive index, n_0, for the transverse plane (90°). The difference in the refractive indices is called the birefringence, B,

$$B = (n_e - n_0), \tag{1}$$

which, in the case of a muscle fibre, is greater than zero. As for nerve (Cohen, Hille & Keynes, 1970), the polarity of the birefringence signals observed will be referred to a longitudinal 'optic axis' (Bennett, 1950) as if the fibre were a uni-axial birefringent structure.

TABLE 1. Relative spectral variation of the output of the photodetector, irrespective of any phase shift introduced before the analyser

λ (nm)	$S(\lambda)$ (%)	λ (nm)	$S(\lambda)$ (%)
370	0·5	603	100
450	19·5	630	86·7
478	29·2	660	69·6
520	64·0	688	73·5
542	95·8	750	11·4
573	99·8	810	0·3

The contractile proteins, in particular the anisotropic A bands, account for most of a fibre's resting birefringence (see review by Huxley, 1957), but other structures, such as the surface and internal membrane systems, must also make a contribution. Approximately two thirds of the resting birefringence of the A bands is due to 'form' birefringence and one third due to 'intrinsic' birefringence (Noll & Weber, 1934).

Operationally, one can directly measure optical retardation, R, which is given by the product of an object's birefringence, B, and thickness, L,

$$R = BL. \tag{2}$$

When referred to the speed of light in a vacuum, optical retardation gives the distance that the slower component of the light lags behind the faster component because of having travelled through the object. The phase shift, ϕ_λ, represents the retardation normalized with respect to a wave-length of light:

$$\phi_\lambda = 2\pi R/\lambda. \tag{3}$$

For a homogeneous birefringent object the intensity of light passed by the analyser to the photodetector, I_λ, depends directly on the phase shift ϕ_λ

$$I_\lambda = k(1 - \cos \phi_\lambda), \tag{4}$$

where k is a constant proportional to the intensity of the light source and the area of the birefringent object from which light is collected (see theoretical curve plotted in Text-fig. 6*A*). This equation is a special case

of the more general situation where the angle, ψ, of the crossed-polarizers with respect to the optic axis of the birefringent object is allowed to take on values other than 45°. Then the dependence of I_λ on ψ and ϕ_λ is described by Fresnel's equation (Cohen *et al.* 1970):

$$I_\lambda = 2k\sin^2(2\psi)\sin^2(\phi_\lambda/2) \quad (5)$$

$$= 4k\sin^2\psi\cos^2\psi(1-\cos\phi_\lambda). \quad (6)$$

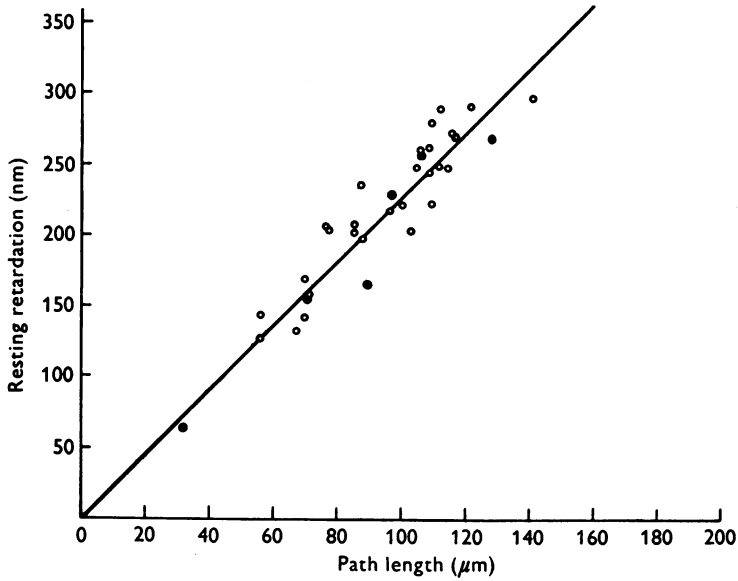

Text-fig. 1. The maximum resting retardation, R_{max}, of a single fibre *vs.* maximum light path length through the fibre. Each symbol represents a different fibre and was the average of two correlated measurements on that fibre. The slope of the line ($2{\cdot}25 \times 10^{-3}$) gives the average birefringence, according to the eqn. $R = B \times L$. A fibre region was routinely selected in which R varied symmetrically over the viewing width and was maximal in the fibre centre. The precise value of R_{max} was then most easily determined by illuminating the middle of the fibre with a narrow longitudinal bar of light. In this case, the visual end-point (a minimal light intensity obtained by varying the amount of retardation introduced by the compensator) is a good deal clearer than when the entire fibre width is illuminated. When measurements of R_{max} were made using this narrow bar technique (filled circles, which are thought to be accurate within $\pm$ 5 nm) and were compared, on the same fibre, with R_{max} measured with the entire width fully illuminated, it was obvious that R_{max} had been systematically over-estimated in the latter method by about 10 %. These latter data (open circles) were therefore corrected for the plot of Text-fig. 2 by scaling the recorded R_{max} by a factor of 0·9. These corrected data are probably accurate only within $\pm$ 3 %. Thus the true value of the average birefringence is known at best within about $\pm\, 0{\cdot}1 \times 10^{-3}$. The average fibre stretch for the measurements was about 1·3 times slack length.

In characterizing the resting retardation of a single muscle fibre and its relationship to the resting light intensity, complications arise because fibre cross-section is not rectangular but more or less elliptical. Thus the retardation, and consequently phase shift (eqn. 3) and light intensity (eqns. 4–6), will vary from edge to centre according to path length (eqn. 2). This point, along with the method for measuring the resting birefringence, is also illustrated in the Plate. Part B shows the same fibre as part A but a variable compensator has introduced -53 nm of retardation to offset the $+53$ nm of retardation in the longitudinal strips of the fibre located near the fibre edge. For light traversing these fibre areas the net retardation at the analyser is zero and these regions therefore appear dark. By further increasing the retardation of the compensator, the resting retardation measured one quarter and three quarters of the way across this fibre's viewing width was determined to be $+227$ nm (part C) and at the middle, where the retardation is maximal, to be about $+302$ nm (part D).

The maximum resting retardation, R_{max}, was determined for thirty-four fibres as a function of the maximum path length through the fibre (path length was determined by rotating the fibre 90° and measuring fibre diameter), with the results plotted in Text-fig. 1. If resting birefringence is distributed according to fibre volume and is constant from fibre to fibre, one would expect the points in Text-fig. 1 to fall on a straight line with slope B, according to eqn. (2). A least-squares straight line constrained to go through the origin gives a satisfactory fit to the data, with the resting birefringence $B \doteq 2{\cdot}25 \times 10^{-3}$. This number is similar to the average birefringence of muscle previously reported in the literature, $2{\cdot}2 \times 10^{-3}$ (Høncke, 1947).

Given B, one can approximate path length, and from this, fibre cross-section, by measuring $R(x)$, fibre retardation as a function of the viewing distance, x, across the fibre width, w. The cross-sectional area, A, for example, should be approximately given by

$$A = \frac{1}{B}\int_0^w R(x)\,dx. \tag{7}$$

This principle is used in connexion with the results presented in Text-figs. 9 and 11 and Tables 3 and 5. For most optical records, the resting retardation was routinely recorded near the edges, half-way from each edge to the centre, and at the centre of the fibre.

Strictly speaking, because of the alternating A and I bands, the resting retardation of a fibre a given distance across its viewing width may not be constant in the longitudinal direction, as is implicitly assumed above. However, if the light path length in the fibre is long enough to include a number of myofibrils which are not precisely in register, the number of A bands intersecting the light path, and thus the

resting retardation will be averaged out in the longitudinal direction. Although this averaging effect is visually apparent in parts *C* and *D* of the Plate, a way to quantitate the extent to which the retardation is uniform in the longitudinal direction is illustrated in Text-fig. 6 (see page 175 for more complete discussion). For this experiment a bar of quasi-monochromatic light illuminated only a narrow strip in the middle of the fibre. The resting light intensity was measured as a function of the variable phase shift introduced in series with the fibre using the compensator. Since these data (open circles, Text-fig. 6*A*) could be closely described by eqn. (4) (continuous trace, Text-fig. 6*A*), the illuminated region behaved as if it had nearly the same resting retardation throughout. At the extreme edges of the fibre, however, where the light path length includes only a few myofibrils, the retardation does not appear visually to be averaged out in this way. For the calculations in the later part of the paper, any longitudinal variations in retardation have been ignored. It is thought that for most fibres, the error introduced because of this is small.

The detailed analysis of Text-fig. 1 was not done for light of wavelengths other than 575 nm. However, an examination of the dependence of B on wave-length was made on one fibre, using the narrow bar of illumination in the fibre middle. Light intensity as a function of variable phase shift was measured by the photodetector for $\lambda = 480$, 570 and 660 nm. These data were then fitted by eqn. (4) (similar to the fit in Text-fig. 6*A*) to determine the best estimate of R_{max} at each wave-length. For the three values of λ, the measurement of R_{max}, and hence birefringence differed by less than 2 %. On this basis B will be assumed to be independent of wave-length.

Properties of the large optical signal preceding contraction

Analogous with the results on nerve (Cohen *et al.* 1970) one expects that light intensity changes recorded with a fibre positioned between crossed polarizers may be related primarily to changes in optical retardation. A retardation change could arise from a change in the product of thickness and birefringence (eqn. 2) of some subcellular structure contributing to the total fibre retardation. However, changes in other optical properties, such as absorption, scattering (Barry & Carnay, 1969; Carnay & Barry, 1969) including diffraction (Hill, 1953), optical rotation, or alignment of optic axis (e.g. the parameter ψ in eqn. (6)), might also contribute to the signals. It is important therefore to perform certain optical tests to see whether the light intensity changes detected are in fact consistent with the view that they arise primarily from changes in optical retardation. This hypothesis concerning the origin of the intensity changes will be referred to as the 'ΔR hypothesis'.

Transmission changes. If, for example, during activity there were a decrease in the fibre's 'transmission' characteristics (the net result of absorption and scattering), one would expect to see a decrease in light intensity passed by the crossed polarizers. The experiment of Fig. 2, on a

fibre in normal Ringer, demonstrates that this mechanism will not explain the main rising phase of the large, early signal. Trace M_1 shows tension, trace O_1 shows the optical signal with crossed-polarizers in place, and trace

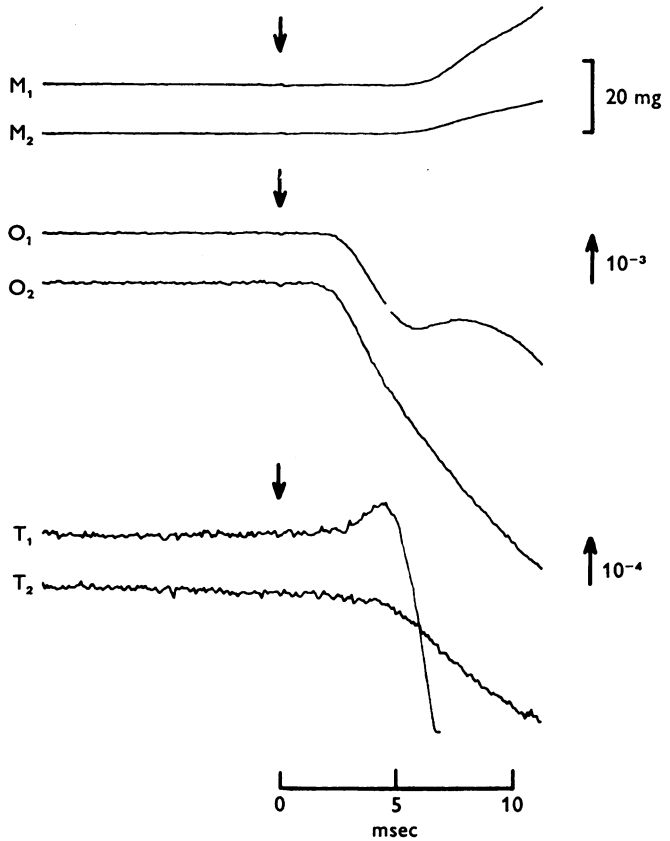

Text-fig. 2. Comparison of mechanical (M), 'birefringence' (O) and 'transmission' (T) signals at different stretch. Subscripts 1 and 2 refer to a fibre stretch of 1·4 and 1·6 times slack length, respectively. R_{max} = 191 nm (recorded for record O_1 only). Iliofibularis m.; average fibre diameter at slack length, 132 μm; light, 570 ± 30 nm; optical recording about 2 mm from cathode; 4 sweeps per trace; DC coupling; temp. 22° C; fibre ref. 072375.01. The optical calibration for the transmission traces has not been corrected for the fact that the fibre filled only about 60 % of the field seen by the photodetector. When referred to light traversing the fibre only, the calibration for traces T_1 and T_2 would be about $1{\cdot}7 \times 10^{-4}$.

T_1 shows the optical signal with the polarizer in place but the analyser removed. In trace T_1 there is apparent a transmission change of similar timing as that of the large, early signal of trace O_1, but it is a much smaller signal and its polarity is wrong to explain the intensity decrease of trace

O_1. A simple transmission change cannot therefore account for the birefringence signal.

These measurements were then repeated on the same fibre, but stretched 1·6 times slack length rather than 1·4. At the higher stretch, the same increase in light intensity without the analyser is no longer present (trace T_2), whereas the intensity decrease with the analyser in place is still large (trace O_2). Although measurements at stretches greater than 1·6 were not made on this fibre, in other experiments the early transmission change was clearly seen to reverse at high stretch and become a small decrease (see, for example, transmission traces, Text-fig. 10). The reason for the reversal with stretch is not understood.

Strictly speaking, to quantitate the size of a pure retardation signal, the intensity change measured with the analyser in place should be corrected for any simultaneously occurring transmission change. Such corrections were not routinely made, but on the basis of experiments like that of Text-fig. 2 using white light, the error involved is thought to be usually less than 10 % for a highly stretched fibre and no greater than about 25 % for a moderately stretched fibre. However, in the analysis of two of the experiments below (Text-figs. 7 and 11) specific corrections for the transmission change were in order.

Evidence that the signal arises from a change in retardation

Some rather specific behaviour is predicted for a light intensity change which arises from a small change in retardation. For each wave-length of light λ and for each narrow longitudinal fibre region of uniform resting retardation R one has

$$\frac{\mathrm{d}I_\lambda}{\mathrm{d}R} = \frac{\mathrm{d}I_\lambda}{\mathrm{d}\phi_\lambda}\frac{\mathrm{d}\phi_\lambda}{\mathrm{d}R}. \tag{8}$$

Therefore from eqns. (3) and (6) it follows that for a small change ΔR in R

$$\Delta I_\lambda = (4k \sin^2\psi \cos^2\psi \sin\phi_\lambda 2\pi/\lambda)\,\Delta R. \tag{9}$$

Angle of incidence, ψ. Eqn. (9) predicts that if the angle of incidence, ψ, that the crossed-polarizers make with the fibre axis is varied, the light intensity change due to a fixed ΔR should simply be scaled by the factor $\sin^2\psi . \cos^2\psi$. For this experiment the same scaling factor applies for any wave-length of light used and for any region of the fibre from which light is collected. Thus, for example, the signal collected from the entire fibre width illuminated with white light should scale as $\sin^2\psi . \cos^2\psi$ under the ΔR hypothesis.

Text-figs. 3 and 4 show the results from an experiment testing the effect of the variable ψ on the magnitude of the large, early signal recorded about

1 mm from the stimulating cathode in normal Ringer. Light of wavelength $\lambda = 570 \pm 30$ nm was used to illuminate the fibre, and the signal was measured from the full fibre width. Text-fig. 3 shows the original records on which the analysis in Text-fig. 4 was done. The theoretical

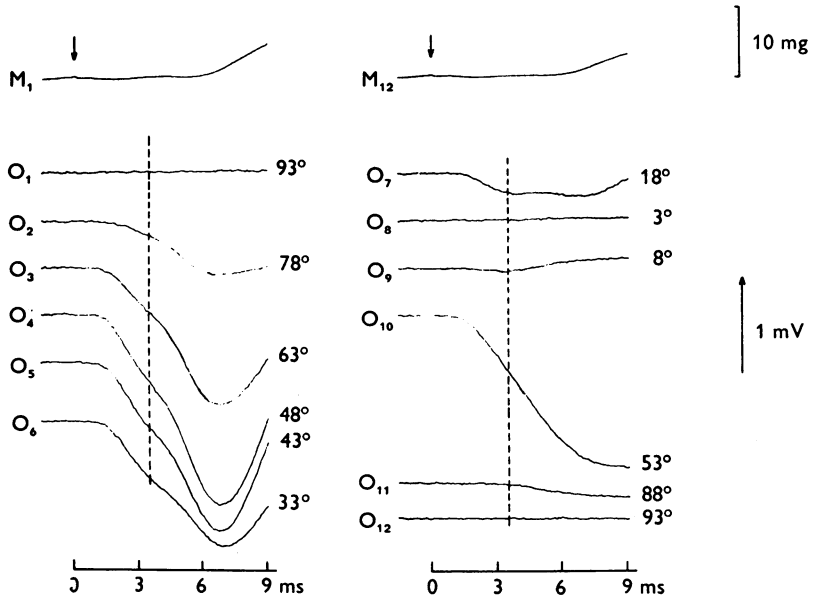

Text-fig. 3. The optical signal as a function of the angle ψ that the crossed polarizers make with respect to the fibre axis. Resting light intensities (mV) for the various optical traces were: O_1 (3 mV), O_2 (88 mV), O_6 (325 mV), O_7 (123 mV), O_8 (4 mV), O_9 (24 mV), O_{10} (357 mV), O_{11} (11 mV), O_{12} (3 mV). Normal Ringer; iliofibularis m.; average fibre diameter at slack length, 95 μm; stretch, 1·36 times slack length; R_{max}, 144 nm; light, 570 ± 30 nm; optical recording 1 mm from cathode; 4 sweeps per trace; DC coupled; temp. 21° C; fibre ref. 071575.01. Data for the analysis of Text-fig. 4 were measured 3·5 ms after stimulation (dashed vertical timing lines).

curves in Text-fig. 4 (continuous traces) are the function $\sin^2\psi.\cos^2\psi$ normalized relative to its maximum value. Two sets of experimental points are also shown as a function of ψ, each set being normalized with respect to the vertical scaling factor which gives the least-squares fit of the data to the theoretical curve: (i) the resting light intensity (open circles, Text-fig. 4*A*) and (ii) the changes in light intensity measured 3·5 ms after the stimulus (filled circles, Text-fig. 4*B*), this time being indicated by the dashed vertical line in Text-fig. 3.

The resting light intensities agree well with the theoretical curve, as one would predict from eqn. (6) and the assumption that the resting fibre behaves essentially as a uni-axial object, with optic axis parallel to the

fibre axis. The changes in light intensity measured 3·5 ms after the stimulus also agree well with the theoretical curve and therefore with the ΔR hypothesis.

Quantitatively similar results were obtained for fibres bathed in mechanically deactivating solutions, D_2O or $2{\cdot}2T$ hypertonic Ringer. In these

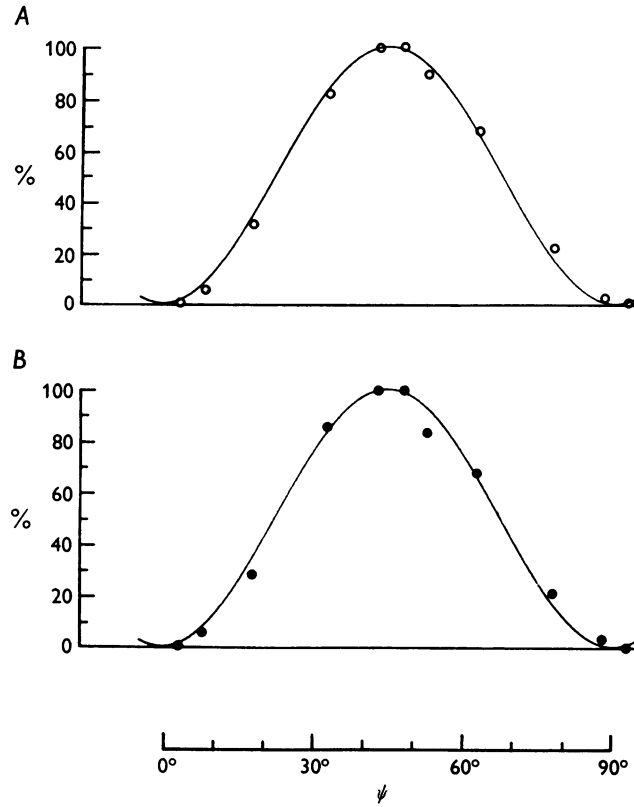

Text-fig. 4. Analysis of angle of incidence experiment shown in Text-fig. 3. *A*, normalized resting light intensities (open circles) as a function of ψ. *B*, normalized changes in light intensity (filled circles, measured 3·5 ms after stimulation) as a function of ψ. The theoretical curve in both parts of the Figure is proportional to the function $\sin^2\psi.\cos^2\psi$ expected under the ΔR hypothesis (see text for further explanation).

cases, however, the theoretical curves could be fitted to the data points measured at the peak of the early signal (about 8–10 ms after stimulation).

Phase shift, ϕ_λ. A second quantitative comparison of the experimental behaviour of the signal with that expected under the ΔR hypothesis is provided by varying the net resting retardation R, and therefore ϕ_λ, preceding the analyser by means of the variable compensator. Under the

conditions of eqn. (9), the change in light intensity due to a constant ΔR should vary as $\sin \phi_\lambda$. Since the factor $\sin \phi_\lambda$ will vary for different wavelengths of light and for fibre regions of different resting retardations, the simplest quantitative approach would be to eliminate this variation by illuminating the fibre with narrow-band light and measuring the signal from a longitudinal fibre strip of uniform retardation.

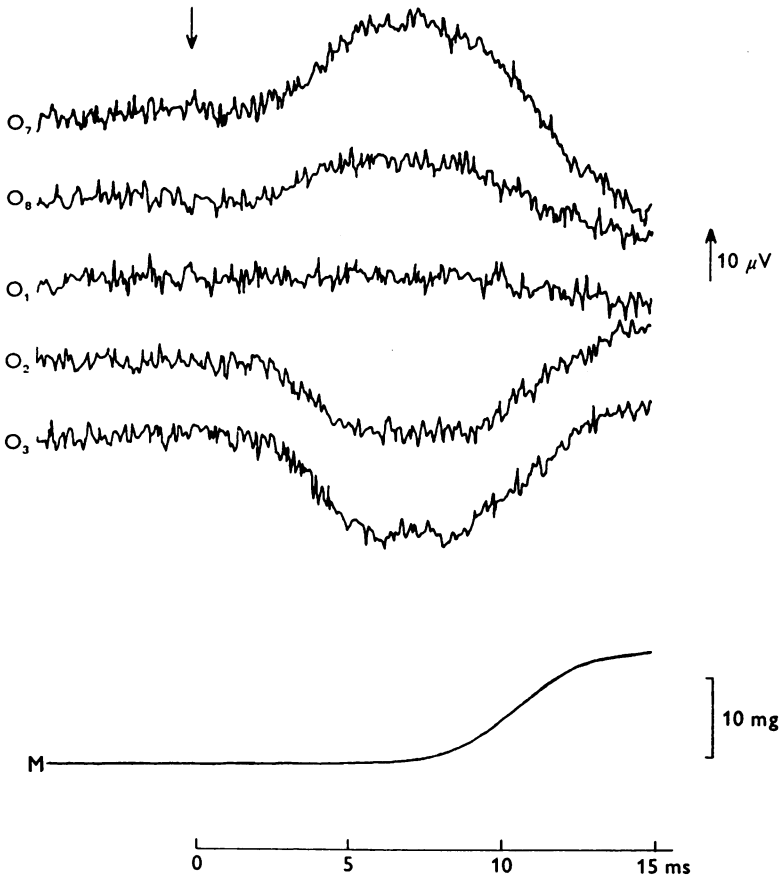

Text-fig. 5. Changes in light intensity (O) as a function of retardation introduced by the variable compensator and mechanical trace (M), for the case of a central longitudinal strip of fibre illuminated with narrow-band light ($\lambda = 575 \pm 15$ nm). Fibre retardation was 270 nm; compensator retardation was: O_1 (-270 nm), O_2 (-193 nm), O_3 (-116 nm), O_7 ($+193$ nm), O_8 ($+270$ nm). Normal Ringer; semitendinosus m.; average fibre diameter at slack length, 200 μm; stretch, 1·69 times slack length; optical recording 2 mm from cathode; 32 sweeps per trace; optical AC coupled, mechanical DC coupled; temp. 23° C; fibre ref. 121274.02.

Results from such an experiment are shown in Text-figs. 5 and 6 for a fibre in normal Ringer. Narrow-band light (575 ± 15 nm), after passing through a horizontal slit in the light path, illuminated a longitudinal region, nominally about 10 μm in width, in the middle of a fibre. Because of light scattering, the effective fibre width illuminated was difficult to determine precisely, but visual observation through an eyepiece in front of the photodiode showed that most of the light was in fact restricted to a

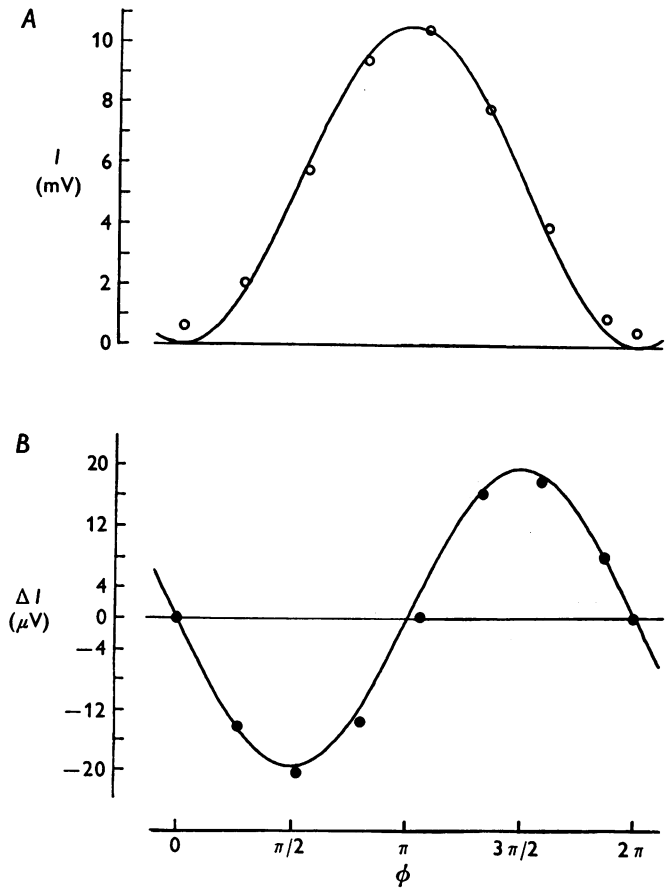

Text-fig. 6. Analysis of full set of records from compensation experiment of Text-fig. 5. *A*, resting light intensities (open circles) as a function of ϕ_λ, the net phase shift of fibre plus compensator. Theoretical curve (continuous trace) is the function $k(1-\cos\phi_\lambda)$, expected if the region of muscle illuminated had a uniform resting retardation of 270 nm. For the curve fit, $k = 5{\cdot}34$ mV. *B*, changes in light intensity (filled circles; measured 7 ms after stimulation) as a function of ϕ_λ. Theoretical curve (continuous trace) is the function $k \sin\phi_\lambda \, \Delta\phi_\lambda$, expected under the ΔR hypothesis. For the curve fit, $\Delta\phi_\lambda = -3{\cdot}65 \times 10^{-3}$ (radians), corresponding to a ΔR of 0·33 nm.

narrow longitudinal region, about 10–15 μm wide, in the fibre centre. The illuminated strip visually appeared to have a uniform resting retardation of about 270 nm. The amount of additional retardation introduced in series with the fibre retardation was then changed in a stepwise fashion by varying the setting on the compensator. The resting light intensity and change in light intensity following stimulation were measured at each setting. The fibre, although stretched to about 1·7 times slack length, was still able to generate some twitch tension and therefore to move slightly following each stimulus. However, as was verified by visual inspection periodically during the experiment, this movement was restricted essentially to the longitudinal direction, with the bar of light remaining focused in the central region of the fibre.

Text-fig. 5 shows a sample of the experimental records obtained and Text-fig. 6 shows the analysis carried out using the full set of records. In Text-fig. 6*A*, the open circles plot the resting light intensity as a function of the net phase shift ϕ_λ of the fibre and compensator in series. Thus the leftmost point corresponds to the compensator having introduced $-2{\cdot}95$ radians of phase shift (-270 nm of retardation at $\lambda = 575$ nm). The continuous trace in Text-fig 6*A* is the function $k(1-\cos\phi_\lambda)$ expected on the basis of eqn (6), where the scaling factor $k = 5{\cdot}34$ mV was determined to give the least-squares fit of the function to the data.

The over-all agreement in Text-fig. 6*A* between the theoretical curve and the experimental data is good, with the possible exception of the two smallest light intensities measured, corresponding to 0 and 1 full wavelength of phase shift. The fact that these light intensities did not extinguish completely with a nominally zero phase shift can reasonably be attributed to light scattering and/or a failure of the illuminated area of the fibre to have exactly the same retardation throughout. The deviation from the theoretical curve is small, however, in support of the assumption that the illuminated region behaved essentially as a birefringent object of uniform retardation (see small print, pp. 167–168).

Text-fig. 6*B* shows the changes in light intensity during activity (filled circles), also plotted as a function of the net resting phase shift ϕ_λ. The intensity changes were measured 7 ms after stimulation, near the peak of the optical signals seen in Text-fig. 5. The continuous curve in Text-fig. 6*B* is the function $k\sin\phi_\lambda\Delta\phi_\lambda$. Under the ΔR hypothesis this function, with k determined from the fit in Text-fig. 6*A*, should fit the measured intensity changes with the vertical scaling factor $\Delta\phi_\lambda$ as the only adjustable parameter. The least-squares fit of this function to the data gave $\Delta\phi_\lambda = -3{\cdot}65\times10^{-3}$ (radians), corresponding to a retardation change 7 ms after stimulation of 0·33 nm. The change in retardation divided by the resting retardation for this fibre strip was therefore $0{\cdot}33/270 = 1{\cdot}22\times10^{-3}$.

The above compensation experiment was repeated for this same fibre but with the narrow slit focused near the edge rather than the middle of the fibre. Because of the cross-sectional curvature at the fibre edge, the resting retardation was, by visual inspection, not constant in the transverse direction within the region of illumination. As one might expect, the resting light intensities and changes in light intensity were not fitted well by scaling the theoretical functions shown in Text-fig. 6.

Because the retardation usually varies greatly over the full fibre width, light intensities measured from the entire fibre in the variable compensation experiment would also be expected to show significant departures from the simple functions $k(1-\cos\phi_\lambda)$ and $k\sin\phi_\lambda\Delta\phi_\lambda$. However, there is one straightforward prediction that can be made under the ΔR hypothesis when illuminating the full fibre width with narrow-band light. If the retardation introduced by the compensator is changed by $\frac{1}{2}$ wavelength, the change in light intensity observed for a pure retardation change should simply be minus the change in light intensity observed without the added compensation. This follows from eqn. (9), since every narrow longitudinal fibre region of uniform phase shift ϕ_λ will then have its contribution to the total light intensity scaled by the same factor, $\sin(\phi_\lambda \pm \pi)/\sin\phi_\lambda = -1$. An experiment showing that the large birefringence signal satisfies this test is given in Text-fig. 10, discussed more fully below.

The above experiments provide strong evidence in support of the ΔR hypothesis but are not conclusive proof of it. Theoretical model systems were investigated in which several objects with varying optical properties were assumed to be positioned in series between crossed-polarizers. Light signals (intensity changes) were generated by introducing a small change in an optical property assumed for one of the objects. The resulting theoretical curves for I and ΔI were compared with those expected under the ΔR hypothesis for the angle of incidence experiment (Text-fig. 4) and compensation experiment (Text-fig. 6). Examples were found which reproduced the experimental relationships expected under the ΔR hypothesis without the underlying mechanism being a change in retardation. However, in contrast to models involving only a change in retardation, such counterexamples were complex and subject to numerous restrictions. The simplest explanation of the results presented in Text-figs. 3–6 is to assume the signal is due to a change in retardation.

Varying the wave-length

As mentioned on page 168, to a good first approximation the resting retardation of a muscle fibre appears to be independent of wave-length in the range λ = 480–660 nm. Similarly, the change in retardation seen in the squid giant axon accompanying a change in membrane potential is approximately independent of wave-length (λ = 400–700 nm; Cohen, Hille, Keynes, Landowne & Rojas, 1971). The experiment shown in Text-fig. 7 was carried out in normal Ringer to investigate the wave-length dependence of the large, early retardation change in muscle.

TABLE 2. Variation of birefringence signal with wave-length, λ

λ (nm) (1)	Trace (2)	ϕ_λ (3)	I (mV) (4)	ΔI (μV) (5)	$\Delta I - S/2$ (μV) (6)	(6) ÷ (4) ($\times 10^{-3}$) (7)
480	Uncompensated	149·7°	24	−28·8	−19·2	−0·80
	Compensated	−30·3°	3*	+9·6		
	$S/2$			−9·6		
570	Uncompensated	126·1°	95	−125·4	−102·6	−1·08
	Compensated	−53·9°	24	+79·8		
	$S/2$			−22·8		
690	Uncompensated	104·1°	64	−102·4	−89·6	−1·40
	Compensated	−75·9°	40	+76·8		
	$S/2$			−12·8		

* This small number may be accurate only within 1–2 mV.

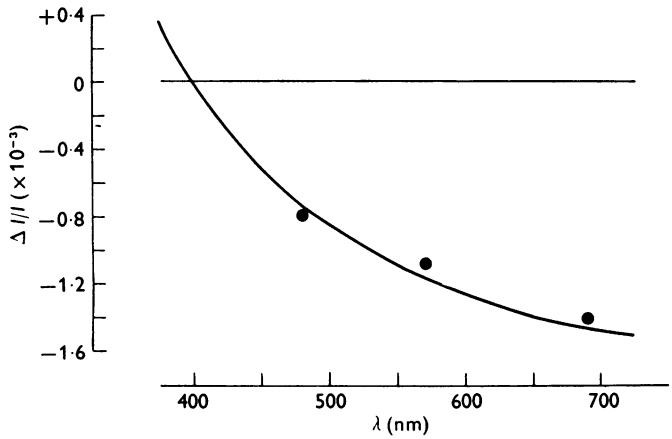

Text-fig. 7. Analysis of optical signal observed from a longitudinal fibre strip of uniform retardation (R = 199·6 nm) as a function of the illuminating wave-length (λ = 480, 570 and 690 nm). See Table 2 for experimental data. At each wave-length, the $\Delta I/I$ plotted (filled circles) has been corrected for the simultaneous 'transmission' change that is assumed to be equivalent to the average component of the signal that does not exactly invert with a half wave-length of compensation. The theoretical curve (continuous trace) describes the relative size of the $\Delta I/I$ to be expected under the ΔR hypothesis, making the additional assumption that ΔR is independent of wave-length. The fit of the theoretical curve to the data involves one adjustable parameter, the scaling factor ΔR, which in the plot has been taken to be 0·205 nm. The fibre for this experiment was in normal Ringer.

As was the case for the experiment of Text-figs. 5 and 6, the theory is simplified if the light is restricted to a fibre region of uniform retardation. A longitudinal strip in the centre of a highly stretched fibre was therefore illuminated with narrow-band light (± 18 nm), using wave-lengths $\lambda = 480$, 570 and 690 nm. Signal-averaged records were taken at each wave-length with first 0° of phase shift introduced by the compensator and then with $-180°$ of additional phase shift. The ΔI was measured in each record 3 ms after the presumed arrival of the peak of the surface action potential. These data are given in column 5 of Table 2. Additionally, at each wave-length the ΔI's of the compensated and uncompensated records were summed and divided by 2 (denoted by $S/2$). Since any pure retardation component of the signal should exactly invert with compensation, the value of $S/2$ should give the size of the non-retardation component of the signal, under the assumption that this latter component has approximately the same magnitude in the compensated and uncompensated traces. This component presumably is caused by the transmission change (see experiment of Text-figs. 10 and 11 discussed below).

If, then, a signal arises purely from a retardation change that is independent of wave-length, the $\Delta I/I$ as a function of wave-length should be given by the ratio of eqns. (6) and (9), i.e.

$$\left(\frac{\Delta I}{I}\right)_\lambda = \frac{\sin \phi_\lambda}{(1-\cos \phi_\lambda)} \frac{2\pi}{\lambda} \Delta R. \tag{10}$$

Since ϕ_λ is available from the resting measurements, ΔR is the only adjustable parameter remaining in eqn. (10). The $\Delta I/I$ of the uncompensated records were in fair agreement with, but showed a systematic deviation from this relationship. However, since the $S/2$ trace at each wave-length was non-zero, the fit of eqn. (10) to the data might be improved by correcting for the presumed transmission change. Column 6 of Table 2 gives the value of $\Delta I - S/2$ for the uncompensated records, these numbers being taken to more closely approximate the pure retardation signal. Column 7 then gives the 'corrected' $\Delta I/I$ at each wave-length. These data are plotted in Fig. 7 (filled circles) and are in significantly better agreement with eqn. (10) (continuous trace) than the uncorrected data (not shown). The value of ΔR chosen for the curve in Text-fig. 7 was 0·205 nm. Thus, when corrected for transmission changes, the experiment supports the idea that the early retardation change is approximately independent of wave-length.

Spatial distribution of the signal across the fibre width

In experiments in which a slit of light was incrementally moved across the viewing width of the squid giant axon (Cohen *et al.* 1970), the retarda-

tion change attributed to the action potential was shown to be maximal at the edges and nearly zero in the middle. This type of spatial distribution is expected for a signal originating from a cylindrical structure with a radially oriented optic axis localized in or near the exterior membrane (Cohen *et al.* 1970). However, since the large, early birefringence signal from a muscle fibre appears to reflect events subsequent to the action potential of the surface membrane, one might expect that the spatial distribution of the signal would have the characteristics of volume not surface. Structures which might give rise to the signal, such as the T system, sarcoplasmic reticulum, myoplasm, or contractile proteins, for example, are all distributed as fibre volume. If the signal is volume-related, the change in retardation measured from a slit of light through the fibre middle might be larger than that measured from the same slit near the fibre's edge by the factor relating the two slices of fibre volume contained in the light path.

Experiments designed to test this hypothesis were carried out in normal Ringer using the small slit of light positioned at various distances across the fibre's viewing width. Of the three such experiments that were successfully completed, all gave the results that (i) the polarity of the initial retardation change, a decrease from resting, was the same no matter which longitudinal region of fibre was being observed and (ii) a relatively large retardation change could be measured from the middle of the fibre. This latter finding is the opposite of that expected for a signal from the surface membrane (Cohen *et al.* 1970). Data and analysis from the fibre which gave the most reproducible results are given in Table 3 and Text-figs. 8 and 9, where light of $\lambda = 575 \pm 15$ nm was used to illuminate the fibre. The optical recordings were made 2 mm from the stimulus cathode to avoid the possible complication of three-dimensional non-uniformities in potential accompanying the shock.

Text-fig. 8 shows the changes in light intensity recorded from the full fibre width (trace O_1) and from five different narrow longitudinal regions equally spaced across the fibre, from lower edge (trace O_2) to upper edge (trace O_6). Trace O_7, the last optical record taken, is from nearly the same position as trace O_2, and shows that the optical measurements were reproducible over time. The tension records as well remained virtually unchanged for the full set of measurements (trace M_1 being taken at the beginning and trace M_7 at the end of the experiment).

Table 3 gives the approximate positions of the five different regions illuminated relative to their viewing width across the fibre (column 3), their average resting retardations (column 4), their corresponding phase shifts (column 5), and their resting light intensities (column 6). Column 7 gives the theoretical resting light intensities predicted for each of the five

TABLE 3. Spatial variation of the birefringence signal

Region no. (1)	Trace no. (Text-fig. 8) (2)	Location (%)* (lower edge = 0%) (upper edge = 100%) (3)	R (nm) (4)	ϕ_λ $\lambda = 575$ nm (deg.) (5)	I (mV) (6)	Predicted I (mV)† (7)	Predicted R (nm) (8)	$-\Delta I$ (μV) (9)	$-\Delta R$ (nm) (10)	Transmission (%) (11)‡
1	O_2	5–15	168	105	9·6	8·9	154	15·1	0·201	88·7
1 repeat	O_7	5–15	176	110	9·6	9·5	154	18·4	0·246	—
2	O_3	25–35	232	145	13·0	12·9	236	8·9	0·200	86·3
3	O_4	45–55	264	165	13·75	14·0	257	6·9	0·346	86·8
4	O_5	65–75	224	140	12·25	12·5	236	9·4	0·188	87·8
5	O_6	85–95	152	95	7·5	7·7	154	7·2	0·093	88·2

* Fibre viewing width was approximately 100 μm; width of bar of light at the fibre was approximately 10 μm.

† Predicted light intensity was determined from the least-squares fit of eqn. (6) to the data of column 5, giving $k = 7{\cdot}1$ mV.

‡ Column 11 gives data taken from a different fibre from that of columns 2–10, using light of $\lambda = 575$ nm.

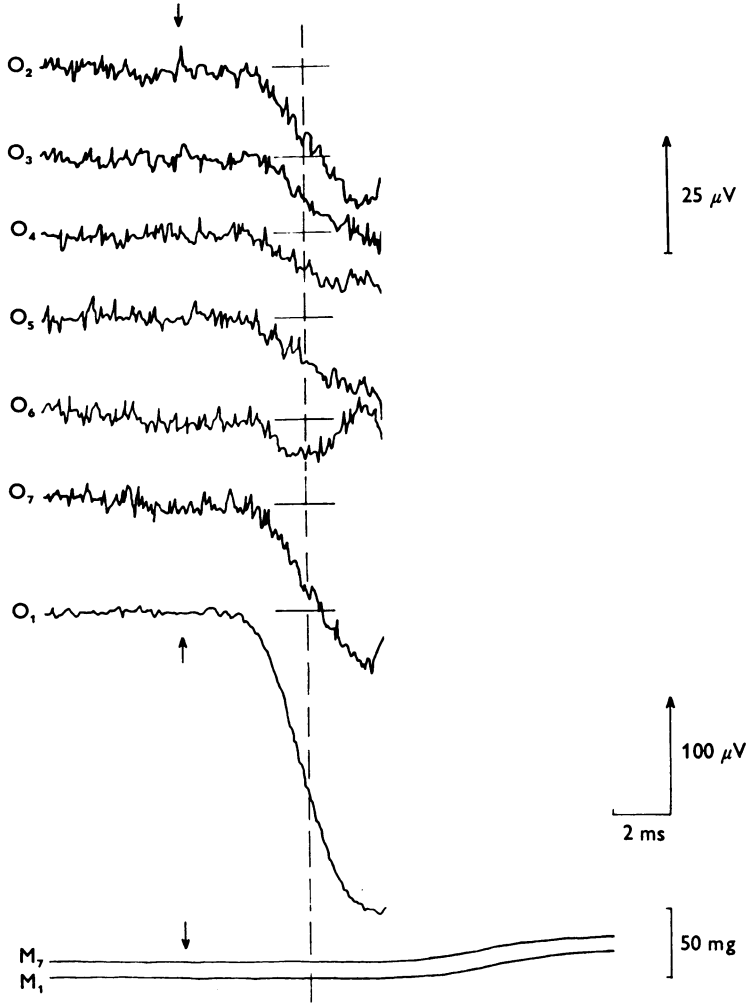

Text-fig. 8. Variation of the optical signal as a narrow bar of light (about 10 μm in width) was moved across the viewing width of the fibre. Optical signals were taken from fibre regions near the lower edge (O_2 and O_7), halfway toward the middle from the lower edge (O_3), at the middle (O_4), halfway toward the upper edge from the middle (O_5), near the upper edge (O_6), and from the entire fibre width (O_1). Resting light intensity for trace O_1 was 180 mV. See Table 3 for resting retardation and resting light intensity of each narrow fibre region. Normal Ringer; semitendinosus m.; average diameter at slack length, 160 μm; stretch, 1·56 times slack length; $\lambda = 575 \pm 15$ nm; optical recording 2 mm from cathode; 16 sweeps per trace for O_1 and M_1, 32 sweeps per trace for all others; optical AC coupled, mechanical DC coupled; temp. 21·5° C; fibre ref. 121274.01. Data for the analysis of Fig. 9 were measured 4·5 ms after stimulation (dashed vertical timing line). Upper optical calibration applies to traces O_2–O_7.

regions on the basis of their measured resting phase shifts and the least-squares fit of the constant k in eqn. (6) to the measured resting light intensities. The agreement between column 6 and column 7 is good, confirming the expectation that the narrow longitudinal regions behave optically as uniform birefringent objects with average phase shifts close to the measured phase shifts.

Under the assumption that the fibre cross-section was elliptical in shape, column 8 gives the resting retardations predicted from eqn. (2) for each of the narrow regions. For this least-squares fit, the locations given in column 3 were used to get a relative light path length, and therefore relative retardation, through the corresponding part of the ellipse. The good agreement between column 8 and column 4 indicates that the fibre cross-sectional shape approximated that of an ellipse, although the orientation of the light path with respect to the axes of the ellipse cannot be determined from these measurements alone. Column 11, which shows data from another experiment, gives the resting transmission characteristics (%) measured from five similar longitudinal regions but with the analyser removed. These data show that a single fibre is quite transparent and that its transmission characteristics differ by less than 5 % over the entire fibre width. Column 9 gives the change in light intensity measured 4·5 ms after stimulation from each fibre region, this time being indicated by the dashed vertical line in Text-fig. 8. Column 10 gives the ΔR corresponding to each ΔI calculated from eqn. (9), column 5, and the constant $k = 7{\cdot}1$ mV determined for the fit of column 7.

The analysis shown in Text-fig. 9 is based on the assumption that the early change in retardation from a fibre strip of homogeneous retardation is a wave form proportional to the fibre volume illuminated This assumption can only be approximately correct, because it ignores the brief propagational delay from the surface membrane into the fibre interior (Gonzalez-Serratos, 1971; Adrian & Peachey, 1973). Since, for each fibre strip of uniform resting retardation, the fibre volume illuminated should be proportional to the light path length through the fibre and therefore to the resting retardation R (eqn. (2)), it follows under this volume hypothesis that

$$\Delta R = cR, \tag{11}$$

where c is a constant.

The open circles in Text-fig 9 plot the retardation change (Table 2, column 10) *vs.* resting retardation (Table 2, column 4) for the different longitudinal strips of fibre illuminated, The open circles, according to eqn. (11), should fall on a straight line intersecting the origin. The continuous line in Fig. 9 gives the least-squares fit of such a line to the data, with the constant c determined to be $-1{\cdot}02 \times 10^{-3}$. Considering the errors involved in assuming a single value of resting retardation for the illuminated strips

near the fibre edge, in making a measurement of resting retardation (estimated as ± 5 nm), and in separating the signals from the noise level there is probably acceptable agreement between the experiment and a volume hypothesis. The dashed theoretical line in Text-fig. 9 follows the theory of

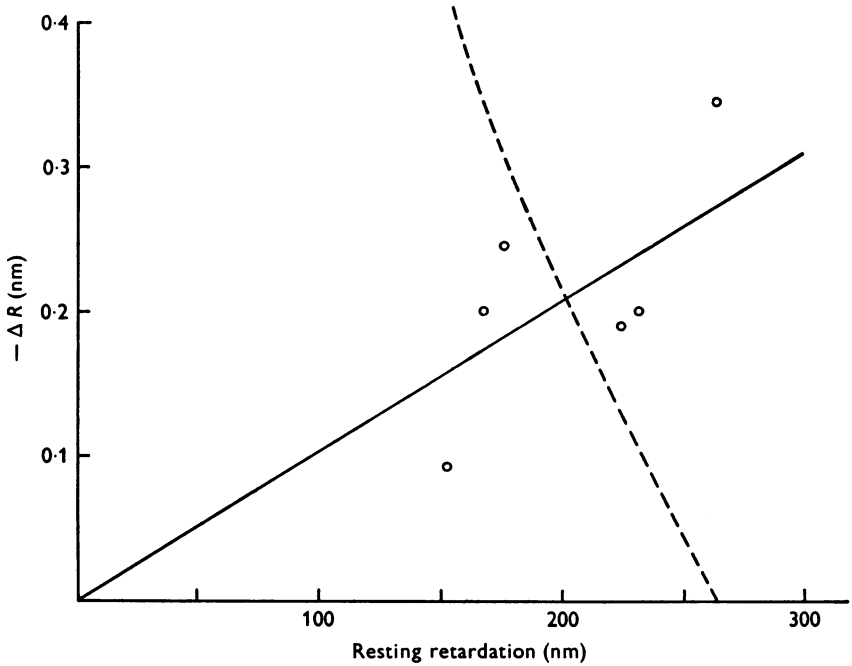

Text-fig. 9. Analysis of spatial experiment shown in Text-fig. 8. Open circles plot the retardation change (Table 3, column 10) measured from each narrow fibre strip 4·5 ms after stimulation as a function of the resting retardation of each region (Table 3, column 4). The straight line through the origin gives the theoretical relationship to be expected if the retardation change is uniformly distributed according to fibre volume. The dashed curve gives the relationship to be expected if the ΔR arises from a surface structure with a radially oriented optic axis. See text for detailed description.

Cohen *et al.* (1970) and indicates the relationship to be expected if the signal arose from a structure with a radially oriented optic axis in or near a cylindrically disposed surface membrane. Clearly the spatial distribution of the rising phase of the large, early retardation change of a muscle fibre is different from a surface-related retardation signal of the type found in the squid giant axon.

In Text-fig. 8 it is apparent that the wave forms recorded from individual fibre regions (traces O_2–O_7) have quite different shapes by the time of the peak of the optical signal collected from the whole fibre (trace O_1). On the face of it, this suggests that the peak of trace O_1 no longer reflects a single, early process, but is likely to be

heavily contaminated by mechanical activity. However, it is probable that the individual traces O_2–O_7 are a good deal more sensitive to the earliest mechanical activity. For example, small shifts in fibre position could cause relatively large shifts in resting retardation for a strip of illuminated fibre, while leaving a signal measured from the entire fibre width relatively unchanged. Thus, trace O_1 could still be reflecting primarily a single process through the time to its peak.

A second experimental approach testing the hypothesis that the large birefringence signal is volume-related is given in Text-figs. 10 and 11. However, for the interpretation of this experiment, as well as the calculations in Tables 5 and 6, it is necessary to have a description of the signal in situations where the wave-length of light and the fibre's resting retardation are not constant.

The birefringence signal summed over distance and wave-length

Suppose the full viewing width, w, of a fibre is illuminated with light of wave-lengths λ_0 to λ_∞, giving rise to a total light intensity, I_T, measured by the photodiode. Let $I(\lambda, x)\,dx\,d\lambda$ be the differential contribution to I_T from a narrow longitudinal strip of fibre located at distance x across the viewing width illuminated by light of wave-length λ, so that

$$I_T = \int_{\lambda_0}^{\lambda_\infty} \int_0^w I(\lambda, x)\,dx\,d\lambda. \tag{12}$$

Now assuming that the resting retardation is constant in the longitudinal direction (see page 167 and Fig. 6*A*) and that differences in the transmission characteristics of the fibre as a function of x are negligible (Table 3, column 11), one has, analogous to eqn. (4), that

$$I(\lambda, x) = kS(\lambda)[1-\cos\phi(\lambda, x)], \tag{13}$$

where $\phi(\lambda, x)$ is the resting phase shift for light of wave-length λ illuminating the fibre strip at distance x across its viewing width. The function $S(\lambda)$ is given in Table 1 and must be introduced to appropriately weight the contribution of each wave-length of light to the total light intensity measured (see Methods for experimental determination of $S(\lambda)$). The constant k is proportional to the absolute intensity of the light source times the length of fibre from which light is collected.

Similarly, let ΔI_T be the total change in light intensity during activity measured from the full fibre width illuminated by light of wave-length λ_0 to λ_∞ and let $\Delta I(\lambda, x)\,dx\,d\lambda$ be the differential contribution to ΔI_T as a function of distance and wave-length, so that

$$\Delta I_T = \int_{\lambda_0}^{\lambda_\infty} \int_0^w \Delta I(\lambda, x)\,dx\,d\lambda. \tag{14}$$

Then, analogous to eqn. (9), one has under the ΔR hypothesis that

$$\Delta I(\lambda, x) = kS(\lambda)\sin\phi(\lambda, x)\,\Delta\phi(\lambda, x), \tag{15}$$

where $\Delta\phi(\lambda, x)$ is the phase shift during activity of the light as a function of distance and wave-length. Hence,

$$\Delta I_T/I_T = \frac{\int_{\lambda_0}^{\lambda_\infty} S(\lambda) \int_0^w \sin\phi(\lambda, x)\,\Delta\phi(\lambda, x)\,dx\,d\lambda}{\int_{\lambda_0}^{\lambda_\infty} S(\lambda) \int_0^w (1-\cos\phi(\lambda, x))\,dx\,d\lambda}. \tag{16}$$

Assuming that the resting retardation $R(x)$ and the change in retardation during activity $\Delta R(x)$ are independent of wave-length (see page 168 and Text-fig. 7), one has

$$\phi(\lambda, x) = R(x)\,2\pi/\lambda \tag{17}$$

and

$$\Delta\phi(\lambda, x) = \Delta R(x)\,2\pi/\lambda. \tag{18}$$

Hence, after substitution

$$\frac{\Delta I_T}{I_T} = 2\pi \frac{\int_{\lambda_0}^{\lambda_\infty} S(\lambda)/\lambda \int_0^w \sin\,(R(x)\,2\pi/\lambda)\;\Delta R(x)\;\mathrm{d}x\,\mathrm{d}\lambda}{\int_{\lambda_0}^{\lambda_\infty} S(\lambda) \int_0^w (1-\cos\,(R(x)\,2\pi/\lambda))\;\mathrm{d}x\,\mathrm{d}\lambda}, \tag{19}$$

where all the terms except $\Delta R(x)$ on the right-hand side of eqn. (19) are known or can be experimentally determined.

Wave-length dependence of the signal from a fully illuminated fibre

The above relationships provide a second way to test the volume hypothesis for the origin of the large, early birefringence signal, Text-figs. 10 and 11. For this experiment the light signal was collected from the full viewing width of a highly stretched fibre in D_2O Ringer.

Text-fig. 10 shows the large signal measured in D_2O Ringer at the extremes of the wave-lengths used (450 nm, left panel; 690 nm, right panel). Optical records were taken either uncompensated (traces O_1 and O_2) or with $\frac{1}{2}$ wave-length of added phase shift (traces O_3 and O_4). At each wave-length the trace labelled $S/2$ is the computer sum divided by 2 of the compensated and uncompensated traces and, as discussed on page 178, approximates the average non-retardation component present in the original records. A small, early signal is apparent on each $S/2$ trace, but the qualitative conclusion is that over the range of wave-lengths used the large, early D_2O signal inverted with compensation, as expected if its optical basis is a change in retardation. Interestingly enough, the uncompensated intensity change for $\lambda = 450$ nm is an increase rather than the usual decrease measured for the large, early signal.

Also shown in Text-fig 10 are the transmission changes (traces T_1 and T_2) measured with the polarizer in place but with the analyser removed. At each wave-length the shape of the transmission trace is nearly superimposable with the corresponding $S/2$ trace. Some uncertainty is associated with comparing the relative magnitude of the two traces, however. This arises in part because, with the analyser removed, the background light intensity is bright and the $\Delta I/I$ of the transmission signal does not refer to light traversing the fibre only. To correct for this, the resting light intensities that apply to the transmission records can be scaled by the proportion of the approximate area of the image field taken up by the fibre. When corrected in this way, the magnitudes of the transmission changes (in terms

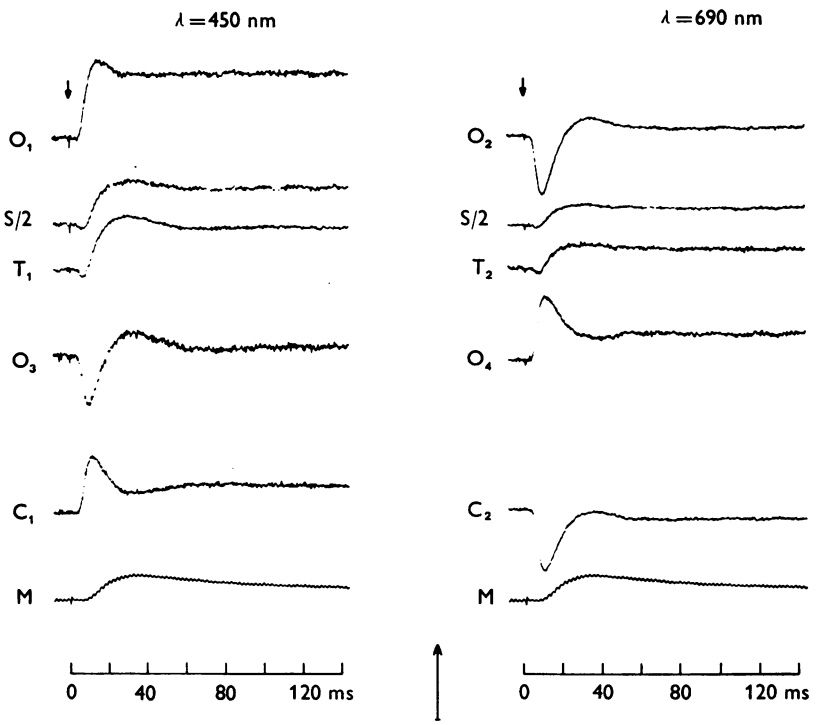

Text-fig. 10. The early birefringence signal collected from the full fibre width as a function of wave-length. Original mechanical (M), birefringence (O), and transmission (T) traces. Illumination for left-hand panel was with $\lambda = 450 \pm 30$ nm and for right-hand panel with $\lambda = 690 \pm 20$ nm. Traces O_1 and O_2 were 'uncompensated' (i.e. the compensator setting was for 0 nm of additional retardation), whereas traces O_3 and O_4 were 'compensated' with $\frac{1}{2}$ wave-length of phase shift (i.e. compensator settings were -225 and -345 nm respectively). At each wave-length the trace labelled S/2 is the computer sum divided by 2 of the compensated and uncompensated traces, and the trace labelled 'C' is the original uncompensated trace minus the S/2 trace. Also shown at each wave-length is the transmission change (traces T_1 and T_2), recorded with the polarizer in place but with the analyser removed. Resting light intensities for the uncompensated records were 0·84 V (O_1) and 2·38 V (O_2). Resting light intensities for the transmission traces were 6·95 V (T_1) and 4·86 V (T_2), of which approximately 43 % was transmitted by the fibre and 57 % was background light. Vertical calibration (large arrow) is 2·36 mg for the mechanical trace and 10^{-3} for all uncompensated birefringence traces, or equivalently 0·84 mV for all traces at $\lambda = 450$ nm (except T_1, for which it is 1·73 mV) and 2·38 mV for all traces at $\lambda = 690$ nm (except T_2, for which it is 1·21 mV). D_2O Ringer; iliofibularis m.; average fibre diameter at slack length, 173 μm; stretched 2·0 times slack length; R_{max}, 304 nm; 3·5 mm from cathode. DC coupling; temp. 23° C; 4 sweeps for each optical trace and 48 for trace M (the latter being displayed at each wave-length). Fibre ref. 042076.01. A sarcomere spacing of 3·9 μm at the site of optical recording was determined by counting the number of sarcomeres in a calibrated distance. Peak switch tension for this fibre in normal Ringer was 189 mg at a stretch of 1·6 times slack length. Small arrows mark moment of stimulation. Experimental records were also obtained at $\lambda = 510$ and 600 nm (not shown).

of $\Delta I/I$) differ by less than a factor of 2 when compared with the magnitudes of the corresponding $S/2$ traces ($\Delta I/I$ referred to the uncompensated state). It therefore appears that the signals in the $S/2$ traces may reasonably be attributed to the transmission change.

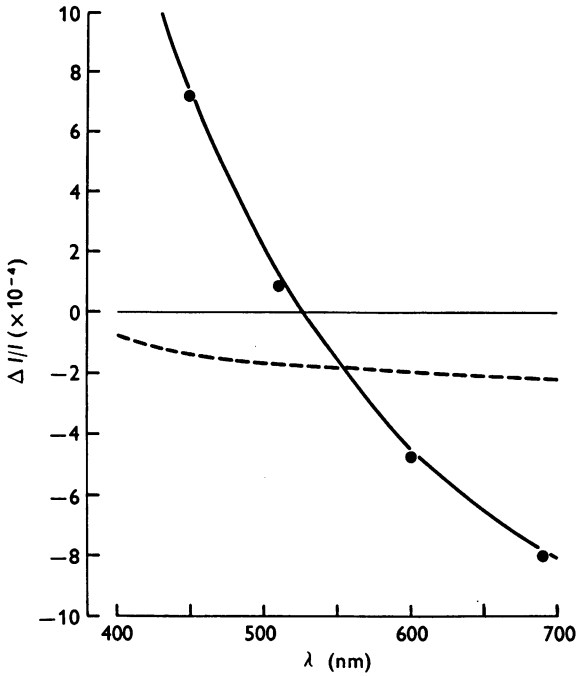

Text-fig. 11. Comparison of volume *vs.* surface hypotheses for the origin of the early birefringence signal. Same experiment as in Text-fig. 10. Data points shown are the magnitudes of the uncompensated traces after correction for the transmission change (e.g. traces C_1 and C_2, Text-fig. 10), measured 10 ms after stimulation. The continuous theoretical curve was derived under the assumption that the retardation change is distributed as fibre volume, whereas the dashed theoretical curve assumes a surface-related signal. A similar analysis of the original uncompensated traces alone (i.e. uncorrected for the transmission change) also supports the conclusion that the signal is volume-related rather than surface-related. However, the fit shown, of the volume-related curve to the 'corrected' data, is a significant improvement over that to the 'uncorrected' data.

At each wave-length in Text-fig. 10 the uncompensated record was therefore corrected for the presumed transmission change by subtracting the corresponding $S/2$ trace. The corrected traces obtained (Text-fig. 10, traces labelled C_1 and C_2) should then more closely approximate that part of the original uncompensated signal that behaves purely as a change in retardation.

The $\Delta I/I$ measured 10 ms after stimulation for these corrected signals, as well as for similarly corrected signals at $\lambda = 510$ and 600 nm, have been plotted in Text-fig. 11 (filled circles). The continuous theoretical curve in Text-fig. 11, giving $\Delta I/I$ as a function of λ, was calculated for the uncompensated signal on the assumption that the signal arises from a retardation change distributed as fibre volume. The dashed curve in Text-fig. 11 is the theoretical relationship to be expected if the retardation change arises from a structure in or near the surface membrane with a radially oriented optic axis. The experimental points are in much better agreement with the continuous curve, providing strong additional support for the hypothesis that the retardation change arises from a structure that is distributed as fibre volume.

The details of calculating the theoretical curves in Text-fig. 11 follow the theory given in eqns. (12)–(19). Assuming an elliptical cross-section and a volume hypothesis

$$R(x) = R_{\max}\left[1-\left(\frac{w/2-x}{w/2}\right)^2\right]^{\frac{1}{2}} \tag{20}$$

and

$$\Delta R(x) = \Delta R_{\max}\left[1-\left(\frac{w/2-x}{w/2}\right)^2\right]^{\frac{1}{2}}, \tag{21}$$

where $R_{\max}$ and $\Delta R_{\max}$ are the resting retardation and change in retardation, respectively, half-way across the viewing width, w, of the fibre. The fact that fibre cross-section was approximately elliptical was verified from the resting retardation measurements across the fibre width (cf. page 182, comments on elliptical shape).

Eqn. (19), after substitution and simplification, then gives

$$\left(\frac{\Delta I_T}{I_T}\right)_\lambda = \frac{2\pi}{\lambda}\frac{\int_0^1 \sin\left(R_{\max}\left(\frac{2\pi}{\lambda}\right).(1-y^2)^{\frac{1}{2}}\right)dy}{\int_0^1\left[1-\cos\left(R_{\max}.\left(\frac{2\pi}{\lambda}\right)(1-y^2)^{\frac{1}{2}}\right)\right]dy}\Delta R_{\max}, \tag{22}$$

where the variable of integration y now corresponds to the fractional distance from the fibre centre towards the fibre edge. According to eqn. (22) the shape of the curve giving $\Delta I_T/I_T$ as a function of λ is determined by the value of $R_{\max}$, whereas $\Delta R_{\max}$ simply serves to scale this shape. For this fibre $R_{\max}$ was 304 nm. The value of $\Delta R_{\max}$, the only adjustable parameter remaining in eqn. (20), was chosen to be $-0{\cdot}266$ nm for the curve fit in Text-fig. 11.

Starting from eqn. (19) a similar approach was used to calculate the surface-related curve. However, in this case $\Delta R_{\max}$, instead of being maximal in the fibre middle and falling to zero at the edges, was assumed to be maximal at the edges and to fall to zero in the middle. The function chosen to approximate this relationship follows the theory of Cohen *et al.* (1970),

$$\Delta R(x) = \Delta R_{\text{surface}} \times \frac{2.n_R^2\left(\frac{w/2-x}{w/2}\right)^2}{n_0\left[n_0^2-n_R^2\left(\frac{w/2-x}{w/2}\right)^2\right]^{\frac{1}{2}}}, \tag{23}$$

where n_0 is the refractive index of the active surface-related structure, n_R is the refractive index of the medium on either side of it, and $\Delta R_{\text{surface}}$ is the only adjust-

able parameter. For the calculation n_R was set equal to 1·34, the refractive index of Ringer, and n_0 to 1·48, the refractive index of membrane (Cohen *et al.* 1970). However, the shape of the theoretical surface curve is rather insensitive to the particular values chosen for n_R and n_0 (as long as $n_0 > n_R$). For calculating the dashed curve in Fig. 11, the value chosen for the scaling factor ($\Delta R_{surface}$) was $-6{\cdot}02 \times 10^{-2}$ nm. $\Delta R_{surface}$ is also not very sensitive to the particular choices for n_R and n_0.

Both theoretical curves in Text-fig. 11 are based on the assumption of a retardation change of constant sign (a decrease) and magnitude that is independent of wave-length. The reason why the uncompensated signal at $\lambda = 450$ nm was an increase in light intensity for this fibre is explained by the volume hypothesis. At this wave-length the resting retardation towards the fibre middle and in series with most of the fibre volume was greater than half a wave-length. The contribution to the signal from this region was therefore an increase in light intensity (see Text-fig. 6 *B*) greater than the decrease in light intensity contributed from the regions in series with the fibre edges, where the resting retardation was less than half a wave-length. In contrast, most of a surface-related signal is assumed to arise from regions near the fibre edges.

Calculation of ΔR per unit path length

Since at least the initial rising phase of the large, early signal in normal Ringer (Text-figs. 8–9) and the peak of the signal in D_2O Ringer (Text-figs. 10 and 11) appears to be a volume-related signal, it is of interest to calculate the magnitude of the retardation decrease normalized by the length of the light path through the fibre. This quantity, denoted ΔR_L, formally has units of (change in) birefringence, but its introduction is not meant to imply that the retardation change could not also involve a change in thickness of the birefringent structure giving rise to the signal. The most straightforward way to calculate ΔR_L is to take measurements from a fibre region of uniform retardation illuminated with narrow-band light, since ΔR can be calculated as was done for the experiments of Text-figs. 5–9, and the path length in the fibre can be estimated from the resting retardation, eqn. (2) and the average value determined for B ($2{\cdot}25 \times 10^{-3}$). Values of ΔR_L ($= \Delta R$/mm) calculated in this way for fibres in normal Ringer are given in Table 4. Column 10 gives the value 2·5 ms after the presumed arrival of the peak of the surface action potential and column 13 gives the value calculated at the apparent peak of the early optical signal.

It is also possible to calculate ΔR_L for the fibres in which the entire fibre width was illuminated, either with narrow-band light or white light. From eqn. (2) it follows that

$$\Delta R(x) = \Delta R_L . R(x)/B \tag{24}$$

and therefore, from eqn. (19), that

$$\Delta R_L = \frac{\Delta I_T}{I_T} \cdot \frac{\int_{\lambda_0}^{\lambda_\infty} S(\lambda) \int_0^w (1 - \cos{(R(x) . 2\pi/\lambda)}\, \mathrm{d}x\, \mathrm{d}\lambda}{\int_{\lambda_0}^{\lambda_\infty} S(\lambda) \int_0^w \sin{(R(x) . 2\pi/\lambda)} \frac{R(x)}{B} \frac{2\pi}{\lambda}\, \mathrm{d}x\, \mathrm{d}\lambda} . \tag{25}$$

Columns 6 and 8 of Table 5 give the values of ΔR_L calculated from eqn. (25) for a number of fibres in normal Ringer illuminated with green light or white light. As for the analysis in Text-fig. 11, $R(x)$ was assumed to conform to an elliptical shape scaled by the maximum retardation (Table 5, column 3) measured at the fibre centre, i.e. to satisfy eqn. (20). A check on this assumption for each fibre was provided by the resting retardation measured half-way from the edges to the fibre centre (Table 5, column 4), which should be 87 % of the maximum retardation. Fibres which did not approximately satisfy this test were excluded from the Table.

TABLE 4. Estimation of ΔR_L from fibre regions of uniform retardation illuminated with green light

Fibre ref. (1)	Stretch (%) (2)	R (nm) (3)	$\phi_\lambda = 575$ (deg.) (4)	I (mV) (5)	K (mV) (6)	$L = R/B$ (mm) (7)	$-\Delta I$ (2·5 ms) (μV) (8)	$-\Delta R$ (2·5 ms) (nm) (9)	$-\Delta R_L$ (2·5 ms) = (9) ÷ (7) (nm/mm) (10)	$-\Delta I$ (peak) (μV) (11)	$-\Delta R$ (peak) (nm) (12)	$-\Delta R_L$ (peak) = (12) ÷ (7) (nm/mm) (13)
120674.01	130	160	100	44·0	37·5*	0·071	12·5	0·031	0·44	21·9	0·054	0·76
120974.02	129	214	134	29·8	17·6	0·095	56·3	0·406	4·27	81·4	0·587	6·18
121274.01	155	263	165	13·75	7·1	0·117	6·94	0·346	2·96	11·3	0·563	4·81
121274.02	170	270	169	—	5·15†	0·120	—	0·200†	1·67	—	0·335†	2·80
010775.01	165	199·6	125	95	59·8‡	0·089	69·8	0·130	1·46	117·0	0·218	2·45
Average ± S.E. of mean									2·16 ± 0·59			3·40 ± 0·85

* Slit size larger than for other fibres.

† Fibre of Text-figs. 5 + 6, ΔR determined from entire curves.

‡ Gain on photodetector increased by 10 times.

TABLE 5. Estimation of ΔR_L from fully illuminated fibre

Fibre ref. (1)	Stretch (%) (2)	R_{max} (nm) (3)	$R_{\frac{1}{4}}/R_{\frac{3}{4}}$ (% of R_{max}) (4)	$-\Delta I$ (2·5 ms)/I ($\times 10^{-3}$) (5)	$-\Delta R_L$ (2·5 ms) (nm/mm) (6)	$\frac{-\Delta I \text{ (peak)}}{I}$ ($\times 10^{-3}$) (7)	$-\Delta R_L$ (peak) (nm/mm) (8)
White light							
071974.01	150	130	74/74	2·93	3·85	3·70	4·87
112774.02	139	160	90/90	0·39	0·57	1·29	1·86
112974.04	135	208	77/77	1·94	3·49	2·58	4·65
120474.01	138	245	88/88	0·39	0·92	0·55	1·29
120974.01	140	137	81/81	2·72	3·64	3·10	4·76
121874.02	171	232	86/86	1·63	3·45	2·30	4·87
011375.01	117	200	96/96	1·28	2·20	1·69	2·90
121974.01	171	208	100/85	1·63	2·93	2·30	4·14
121274.02	169	270	89/89	0·54	1·69	0·63	1·98
072675.01	150	108	81/81	1·33	1·66	2·32	2·90
121874.01	179	238	81/81	0·76	1·69	1·52	3·38
072475.01	158	173	79/79	1·40	2·12	3·20	4·85
121174.01	164	288	83/83	0·73	3·05	1·41	5·90
071675.02	133	173	83/83	1·16	1·76	3·20	4·86
072175.01	150	216	81/81	0·60	1·13	1·00	1·89
072175.02	150	191	93/93	1·10	1·80	1·32	2·17
072275.02	133	158	75/75	0·59	0·84	*	*
072375.02	133	243	73/73	1·90	4·41	3·12	7·25
072675.02	164	137	82/82	1·35	1·81	1·99	2·67
Average					2·26 ($n = 19$)		3·70 ($n = 18$)
Green light (λ_{peak} = 570 nm)							
072475.03	150	144	78/78	1·35	1·85	*	*
071875.03	158	173	69/69	1·90	2·87	3·17	4·80
121274.01	156	264	88/85	0·98	2·84	1·42	4·11
Average					2·52 ($n = 3$)		4·46 ($n = 2$)
Overall average ± S.E. of mean					2·30 ± 0·22		3·78 ± 0·34

* Signal did not reach a distinguishable peak or plateau.

TABLE 6. Estimation of peak ΔR_L in D_2O Ringer

Fibre ref. (1)	Stretch (%) (2)	Light (3)	R_{max} (nm) (4)	$R_{\frac{1}{4}}/R_{\frac{3}{4}}$ (% of R_{max}) (5)	$\frac{-\Delta I \text{ (peak)}}{I}$ ($\times 10^{-3}$) (6)	Time-to-peak (ms) (7)	$-\Delta R_L$ (peak) (nm/mm) (8)
072475.02	158	White	194	74/74	0·88	8·6	1·47
072475.03	170	White	151	74/74	1·13	9·1	1·58
042076.00	200	690 ± 20	304	87/87	0·80	10·0	2·01
072675.01	150	White	170	69/69	1·00	9·9	1·50
072675.02	164	White	135	78/78	0·83	6·6	1·11
Average ± S.E. of mean							1·53 ± 0·13

The calculated values of ΔR_L are directly proportional to the value assumed for the resting birefringence B. Estimates of B in D_2O Ringer compared with normal Ringer indicated approximately no change for two fibres and an increase in B of 25 % for a third fibre. For the calculations in Table 6, B has been set equal to its average value determined in normal Ringer, i.e. $2{\cdot}25 \times 10^{-3}$.

The average values of ΔR_L determined by the method of eqn. (25) are in good agreement with the average values given in Table 4, both when measured 2·5 ms after the presumed peak of the surface action potential and at the apparent peak of the early optical signal. The earlier of the two measurements should give, on the average, about the largest change that behaves by all the experimental criteria as a relatively pure retardation change. The peak measurement, in many fibres, is likely to be complicated by mechanical activity, but in the case of a highly stretched fibre may still reflect primarily a single process.

From the average resting birefringence B, the figures in Table 5 for ΔR_L can be used to obtain, by eqn. (24), average values for the fractional decrease in retardation due to the early process compared with the resting retardation. These values are $1{\cdot}02 \times 10^{-3}$ (2·5 ms after surface action potential) and $1{\cdot}68 \times 10^{-3}$ (apparent peak).

Table 6 gives the results of the same calculation for ΔR_L for the D_2O signal measured at its peak. The average peak value of ΔR_L from Table 6, 1·66 nm/mm, is approximately 45 % of the magnitude of, and in general occurred 3–4 ms later than, the average peak ΔR_L seen in normal Ringer.

DISCUSSION

The experiments of this paper show that the large, early optical signal reported previously (Baylor & Oetliker, 1975, 1977*a*) is very likely due to a small decrease in optical retardation, about 1 part in a 1000, compared with the fibre's resting retardation. This retardation change appears to be independent of wave-length (for λ between 480 and 690 nm) and distributed as fibre volume.

The early retardation change and the early transparency change

An early transparency change in whole frog muscle, beginning possibly as early as the earliest detectable length change of latency relaxation, was first reported by Schaefer & Göpfert (1937) and by Buchtal, Knappeis & Sjöstrand (1939). Hill (1949) confirmed the existence of this signal, and later (Hill, 1953) showed that the early intensity change he measured was due to a small decrease in diffraction. Carnay & Barry (1969) and Barry & Carnay (1969) have also reported a transparency change detectable early in the latent period that appeared to be due to a simple scattering change, however, rather than a change in diffraction.

The large, early birefringence signal clearly overlaps the time of these early transparency changes. Measurements on the same single fibre confirm that an early transparency change can usually be detected beginning nearly simultaneously with the large, early birefringence signal (Text-figs. 2 and 10). Whether or not these optical signals all reflect primarily the same underlying process is not known. Interestingly enough, in a single fibre, the birefringence signal appears relatively uncomplicated by, and has a much larger signal-to-noise ratio than the transparency change.

The reduced magnitude of the early birefringence signal in mechanically deactivating solutions and with stretch

It is likely that the large, early birefringence signal reflects some change taking place within the fibre volume linking excitation to contraction (see also Discussion of Baylor & Oetliker, 1977*b*). The reduced magnitude of the signal with high stretch or after replacement with D_2O or hypertonic Ringer (Baylor & Oetliker, 1977*a*) may therefore reflect some decreased physiological activity, such as a reduced amount of Ca^{2+} released from the sarcoplasmic reticulum. Alternatively, this reduction might be the result of a change in fibre geometry or in some physiologically irrelevant optical property of the fibre. For example, since a single fibre shrinks in hypertonic Ringer, one could expect that its birefringence B would also change and this in turn might affect the size of the measured intensity changes, independent of a significant change in any physiological step leading up to the activation of contraction. The simplest situation in this case would be for B to be proportional to the concentration of the birefringent material. Hence, when fibre volume decreased from V to V', the birefringence might increase from B to B' according to

$$B'/B = V/V'. \tag{26}$$

The approximate change in volume expected for a single fibre held isometrically as the tonicity is raised has been determined by Blinks (1965):

$$V'/V = 0{\cdot}34 + 0{\cdot}66/T, \tag{27}$$

where T is the new tonicity relative to isotonic. In the idealized case of a circular fibre cross-section decreasing from radius a to $a' = a(V'/V)^{\frac{1}{2}}$, the maximal retardation measured at the fibre centre, R_{max}, might then increase to R'_{max} according to

$$\frac{R'_{max}}{R_{max}} = \frac{B'.(2a')}{B.(2a)} = \left(\frac{V}{V'}\frac{a'}{a}\right) = \left(\frac{V}{V'}\right)^{\frac{1}{2}} \tag{28}$$

$$= (a/a'). \tag{29}$$

Although a systematic determination of B in the various hypertonic Ringer solutions used was not made, as was done for fibres bathed in isotonic Ringer (Text-fig. 1), measurements of resting retardation on a number of fibres in 2·2–3T Ringer indicated that R_{max} usually increased as volume decreased but not quite as much as predicted by eqns. (26)–(29). For example, the typical changes observed when tonicity was increased from isotonic into the range 2·2–3T were that the fibre viewing width (and resting light intensity) decreased by about 10–20 % whereas the maximum resting retardation increased rather less, usually between 0 and 10 %. A

departure from eqn. (29) in this direction might have been anticipated because, as the average refractive index of the medium surrounding myosin increases with tonicity towards that of myosin, the form birefringence of the fibre should probably increase less than the simple case treated by eqn. (26). However, the effect of these tonicity increases on the resting birefrigence other than predicted by eqns. (26)–(29) appears to be rather small. Now if tonicity has about the same relative effect on the change in retardation which gives rise to the large, early optical signal as it does on the resting retardation (as might be the case if the signal depended on a changing property of either form or intrinsic birefringence), one would expect the ΔI of the signal to decrease slightly and the $\Delta I/I$ perhaps not at all as tonicity increased from 1 to $3T$. Experimentally, however, the $\Delta I/I$ of the large signal usually fell by a factor of about 50 (Baylor & Oetliker, 1975). On this basis, it seems likely that the steep decline in the early optical signal with tonicity reflects some decreased physiological activity. The increase in time to peak of both the optical and mechanical signals with increasing tonicity (Baylor & Oetliker, 1977*a*) is additional evidence that the change in appearance of the large, early signal reflects some changing physiological activity.

Similar arguments regarding the physiological significance of the reduced and delayed birefringence signal with high stretch and D_2O replacement can also be made, but in general the magnitudes of these effects are quantitatively less convincing than the hypertonic Ringer case discussed above. In particular, the reduction of the optical signal with high stretch, which was usually about a factor of 2, may be consistent with a minor geometrical or optical change not necessarily related to changes in physiology.

Size of the retardation change if referred to the SR membrane

It has been suggested previously (Baylor & Oetliker, 1975), that one possible source of the large, early retardation change is a potential change across the sarcoplasmic reticulum membranes associated with the release of Ca^{2+}. If it is assumed that the retardation change primarily arises from the membrane of the sarcoplasmic reticulum, one can, making assumptions about the quantity and disposition of this membrane, use the results from Tables 4–6 for ΔR_L to arrive at a tentative figure for the retardation change normalized with respect to a single thickness of the membrane, ΔR_{SR}. This 'membrane parameter' may then be compared with values, measured for other active membranes (cf. Cohen *et al.* 1970; Baylor & Oetliker, 1977*b*). For this calculation a value of $3{\cdot}7 \times 10^3$ mm^{-1} will be assumed for the ratio of sarcoplasmic reticulum membrane area to fibre volume. This figure is an average value reported from morphological studies: $5{\cdot}4 \times 10^3$ mm^{-1} (Peachey, 1965) and $2{\cdot}0 \times 10^3$ mm^{-1} (Mobley &

Eisenberg, 1975). It will also be assumed that the net amount of sarcoplasmic reticulum membrane oriented in the longitudinal direction is 64 % (Mobley & Eisenberg, 1975). Since in cross-section this net amount of longitudinally disposed membrane should have no further preferential orientation, it should have the same angular distribution as a right circular cylinder of membrane.

To evaluate ΔR_{SR}, then, consider a narrow longitudinal region of fibre of width Δx mm illuminated by light with a path length through the fibre of distance r mm. The change in retardation of the light from this region during activity is $\Delta R = \Delta R_L r$ and the region illuminated contains the equivalent of $(0{\cdot}64)(3{\cdot}7 \times 10^3) r/\pi$ right circular cylinders of sarcoplasmic reticulum membrane of diameter Δx mm. Thus

$$\frac{\Delta R}{(0{\cdot}64)(3{\cdot}7 \times 10^3)(r/\pi)} = 1{\cdot}33 \times 10^{-3} \Delta R_L$$

gives the retardation change referred to a single right circular cylinder of membrane of diameter Δx mm. As such, this latter figure really represents the retardation change of a cylindrically disposed structure averaged over the width Δx mm. Assuming the active structure has a radially oriented optic axis, the factor 1·18 can then be derived from the theory of Cohen *et al.* to convert the average retardation change measured from a single right circular cylinder of membrane to the retardation change referred to a single thickness of that membrane (see Fig. 10 of Cohen *et al.* 1970). Hence

$$\Delta R_{SR} = 1{\cdot}18 \times 1{\cdot}33 \times 10^{-3} \Delta R_L, \tag{30}$$

where ΔR_{SR} is in nm if ΔR_L is in nm/mm. Accordingly, in normal Ringer the estimate of ΔR_{SR} 2·5 ms after the peak of the surface action potential is $-3{\cdot}6 \times 10^{-3}$ nm and at the apparent peak of the early process is $-5{\cdot}9 \times 10^{-3}$ nm. In D_2O Ringer the estimate of the peak ΔR_{SR} is $-2{\cdot}4 \times 10^{-3}$ nm.

Further discussion of the sarcoplasmic reticulum hypothesis compared with other possibilities for explaining the large, early birefringence signal is given in the following paper (Baylor & Oetliker 1977*b*), after presentation of the results concerning retardation changes from surface and *T*-system membranes.

This work was supported by a grant from the U.S. National Institutes of Health to Dr W. K. Chandler (whom we thank for encouragement and much helpful advice throughout the course of this work) and by research funds of the Schule für Biologie Laboranten, Wander, and of the Physiologisches Institut der Universität Berne. We also thank Mr H. Fein and Staff and Mr C. Cigada (for technical assistance), Dr L. B. Cohen and Professor A. von Muralt (for helpful advice and loan of equipment), and Drs R. W. Tsien and D. Campbell (for suggestions on the manuscript). S.M.B.'s visit to Switzerland was supported by a grant from the Roche Research Foundation for Scientific Exchange and Biomedical Collaboration with Switzerland.

REFERENCES

ADRIAN, R. H. & PEACHEY, L. D. (1973). Reconstruction of the action potential of frog sartorius muscle. *J. Physiol.* **235**, 103–131.

BARRY, W. H. & CARNAY, L. D. (1969). Changes in light scattered by striated muscle during excitation–contraction coupling. *Am. J. Physiol.* **217**, 1425–1430.

BAYLOR, S. M. & OETLIKER, H. (1975). Birefringence experiments on isolated skeletal muscle fibres suggest a possible signal from the sarcoplasmic reticulum. *Nature, Lond.* **253**, 97–101.

BAYLOR, S. M. & OETLIKER, H. (1977*a*). A large birefringence signal preceding contraction in single twitch fibres of the frog. *J. Physiol.* **264**, 141–162.

BAYLOR, S. M. & OETLIKER, H. (1977*b*). Birefringence signals from surface and T-system membranes of frog single muscle fibres. *J. Physiol.* **264**, 199–213.

BENNETT, H. S. (1950). The microscopical investigation of biological materials with polarized light. In *McClung's Handbook of Microscopical Techniques*, ed. JONES, R. M., 3rd edn. New York: Hoeber.

BLINKS, J. R. (1965). Influence of osmotic strength on cross-section and volume of isolated single muscle fibres. *J. Physiol.* **177**, 42–57.

BUCHTAL, F., KNAPPEIS, G. G. & SJÖSTRAND, T. (1939). Optisches Verhalten der querstreiften Muskelfaser im natürlichen Licht. *Skand. Arch. Physiol.* **82**, 225–257.

CARNAY, L. D. & BARRY, W. H. (1969). Turbidity, birefringence, and fluorescence changes in skeletal muscle coincident with the action potential. *Science, N.Y.* **165**, 608–609.

COHEN, L. B., HILLE, B. & KEYNES, R. D. (1970). Changes in axon birefringence during the action potential. *J. Physiol.* **211**, 495–515.

COHEN, L. B., HILLE, B., KEYNES, R. D., LANDOWNE, D. & ROJAS, E. (1971). Analysis of the potential-dependent changes in optical retardation in the squid giant axon. *J. Physiol.* **218**, 205–237.

GONZALEZ-SERRATOS, H. (1971). Inward spread of activation in vertebrate muscle fibres. *J. Physiol.* **212**, 777–799.

HILL, D. K. (1949). Changes in transparency of muscle during a twitch. *J. Physiol.* **108**, 292–302.

HILL, D. K. (1953). The effect of stimulation on the diffraction of light by striated muscle. *J. Physiol.* **119**, 501–512.

HØNCKE, P. (1947). Investigations on the structure and function of living, isolated, cross-striated muscle fibres of mammals. *Acta physiol. scand.* **15**, suppl. 48.

HUXLEY, A. F. (1957). Muscle structure and theories of contraction. *Prog. Biophys. biophys. Chem.* **7**, 255–318.

MOBLEY, B. A. & EISENBERG, B. R. (1975). Sizes of components in frog skeletal muscle measured by methods of stereology. *J. gen. Physiol.* **66**, 31–45.

NOLL, D. & WEBER, H. H. (1934). Polarisationsoptik und molekularer Feinbau der Q-Abschnitte des Froschmuskels. *Pflügers Arch. ges. Physiol.* **235**, 234–246.

PEACHEY, L. D. (1965). The sarcoplasmic reticulum and transverse tubules of frog's sartorius. *J. cell Biol.* **25**, 209–231.

SCHAEFER, H. & GÖPFERT, H. (1937). Aktionsstrom und optisches Verhalten des Frosch muskels in ihrer zeitlichen Beziehung zur Zuckung. *Pflügers Arch. ges. Physiol.* **238**, 684–708.

EXPLANATION OF PLATE

Fibre as viewed in polarizing microscope, either uncompensated (*A*) or with -53 nm (*B*), -227 nm (*C*), or -302 nm (*D*) of retardation introduced by the compensator. Black regions indicate where the net phase shift at the analyser is zero. Illumination with light of wave-length $\lambda = 544$ nm. Essentially the same features as illustrated in the Plate are seen with the fibre mounted in the micro-optical bench, although with somewhat less resolution compared with the polarizing microscope.

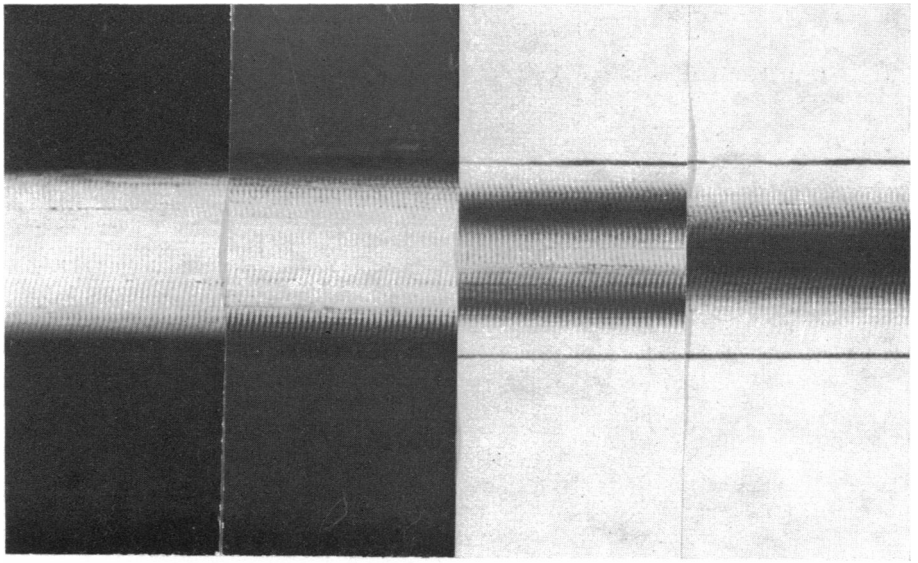
A
B
C
D